

# Biogenic Ag-Ni Bimetallic Nanoparticles from *Croton blanfordianum* L and their Biological Applications

Ravi Chandra Gurrula<sup>1</sup>, J. Prem Chand<sup>1</sup>, M. Padma<sup>1</sup>, N. Annapurna<sup>1</sup>, S. Aruna Kumari<sup>3</sup>,  
Ch. Jogi Narayana<sup>1</sup>, B. Swarna Latha<sup>2</sup>, Kishore Babu Bonige\*

<sup>1</sup>Department of Engineering chemistry, Andhra University, Visakapatnam.

<sup>2</sup>Department of Physics and Engineering Physics, Andhra University, Visakhapatnam

<sup>3</sup>Department of Chemistry, Aditya Engg College, Surampalem

\*Corresponding Author: E – Mail ID: jacobkishore@gmail.com

## ABSTRACT

An environmentally friendly and economical method was reported for green synthesis of Ag-Ni bimetallic nanoparticles by using *Croton blanfordianum* L leaf extract. The phyto molecules present in the extract are acting as reducing agents, stabilizing and capping agents for the biosynthesized nano particles. The characterization studies were done by UV-VIS, FTIR spectroscopies, SEM, EDX, XRD, BET and HRTEM analyses. These BMNPs also showed inhibition of the *Mycobacterium tuberculosis* by using Alamar blue dye in the lowest concentration range of >12.5 µg/ml.

**KEY WORDS:** Bimetallic nanoparticles (BMNPs), *Croton blanfordianum* L (CB).

## 1. INTRODUCTION

Nanotechnology is one of the most exciting disciplines in science, with nanotechnology receiving the majority of the continuing arguments, definitions, and research attention. Nanotechnology is a subgroup of technology that comprehends the study of phenomena at the nanoscale and is found in colloidal science, chemistry, physics, biology, and other scientific subjects (Mansoori and Soelaiman, 2005). Nanotechnology is defined as any technology that operates on the nanoscale of the range (1-100nm) and has applications in the real world, i.e., employing single atoms and molecules to construct functional structures (Kaehler, 1994). Nanotechnology is the study and use of chemical, physical, and biological systems with structural properties ranging from single atoms or molecules to sub-micron dimensions, as well as the integration of the resulting nanostructures into real-world systems (Daniel and Astruc, 2004). In recent times bimetallic nanoparticles have gained considerable attention because of their importance for magnetic, optical and catalytic applications in multiple fields (Venkatesan and Santhanalakshmi, 2011; Srinoi, 2018). There are numerous methods available by taking various ways for the synthesis of nanomaterials. The chemical methods are mostly used for nanomaterial synthesis due to its less time consumption for synthesis of high quantity of nanomaterials. Furthermore, chemical reagents commonly used for synthesis and also for the stabilization of nanoparticles which are hazardous and can lead to harmful byproducts that are not environmentally benevolent (Pantidos, 2014; Shah, 2015).

The demand for eco-friendly non-hazardous methods for the synthesis of nanomaterials is a growing demand in biosynthetic approaches which are not involved in the consumption of toxic chemicals as by-products. A variety of natural sources are there for the synthesis of metal nanomaterials including plants, algae, actinomyces, yeast, bacteria and fungi, etc. (Park, 2011). The bio-mediated synthesis of noble nanometals (Au, Pt, and Ag nanoparticles) by using fungi, bacteria, algae, and also from different parts of plants viz roots, leaves, flowers, stems, etc has gained more significance as a safe alternative so more preferable than physical methods and chemical procedures (Lee, 2014).

Synthesis of nanomaterials by taking plant extract is cost-effective, eco-friendly, and effortless. Therefore it can be used as a valuable and budget-friendly alternative for the production of metal nanoparticles. The bio reduction of metals by combinations of Phyto molecules present in extracts of plants such as phenols, amides, sterols, flavonoids, terpenes, carbohydrates, and amino acids is environmentally benign involving green procedure (Koduru, 2018; Maksakova, 2020; Greer and Nix, 2006).

*Croton bonplandianum* L is found in South Western Brazil, Northern Argentina, Paraguay, Southern Bolivia, and India. It belongs to the *Euphorbiaceae* family is a small annual herb commonly known as Bana Tulasi or Kala Bhangra. As reported, *Croton bonplandianum* L has several medicinal usages and also shows insect repellent properties (Jeeshna, 2011). *Croton bonplandianum* L was also shown to exhibit antibacterial (Parthiban, 2021), antifungal, antioxidant (Divya, 2011), analgesic (Sahoo, 2010), nematicide, anticoronary (Chande, 2011), hepatoprotective, and wound healing properties (Srideshpande, 2018).

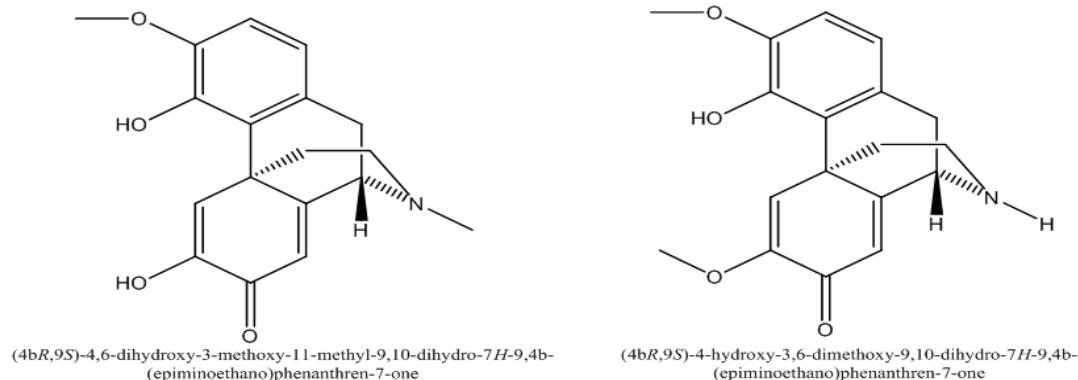


**Figure.1. Major Chemical constituents identified in *Croton bonplandianum L* leaves**

The contemporary antimycobacterial-drug dilemma and the position of tuberculosis (TB) as a major worldwide health problem are largely due to the rapid rise of combative, multidrug-resistant Mycobacteria strains. The limited production of recently licensed antibiotics leads to the present research interest on alternate bacterial compounds, including such improved materials. Nanotechnology and nanoparticle research has yielded a slew of novel concepts and tactics that could prove to be helpful aids in the fight against tuberculosis. A new antituberculous therapeutic paradigm based on silver nanoparticles has the potential to overcome the medical restrictions placed on TB treatment by drug resistance, which has been observed for the majority of conventional organic antibiotics.

Silver NPs are undeniably intriguing prospective medicines for the treatment of mycobacterial-induced illnesses, but their practicality hinges on resolving many key therapeutic challenges, including inadequate transport, inconsistent intramacrophagic antimycobacterial efficacy, and residual toxicity. We present an overview of the pathology of mycobacterial-induced diseases in this work, as well as the benefits and drawbacks of Ag nanoparticles (AgNPs) in TB treatment.

## 2. EXPERIMENTAL

**Materials:** Chemical reagents used (silver nitrate ( $\text{AgNO}_3$ ), nickel nitrate ( $\text{Ni}(\text{NO}_3)_2$ ), ammonium hydroxide ( $\text{NH}_4\text{OH}$ ), Hydrochloric Acid ( $\text{HCl}$ ), Glycerol, OADC (Oleate Albumin Dextrose Catalase), DMSO, Almar Blue) in this study were of analytical grade. Deionized water was used to clean glassware, to prepare chemical solutions and for experimental procedure. Fresh leaves of *Croton bonplandianum L* was collected from the barren lands in and around Lakshmiapuram village in Jeelugumelli Mandal of West Godavari district in the Andhra Pradesh state of India, where it was found naturally.

**Preparation of leaf extract:** The leaves were separated from the branches and washed properly under running piped water two times to remove dust, debris, and other impurities and then with double distilled water two times. Now, these leaves were made to dry under shade for 7 days and these leaves were sliced into tiny pieces and made powder by using the home blender. The obtained powder was kept in an airtight container at  $4^\circ\text{C}$  in a refrigerator for further usage (Selvamangai, 2012). Collections were made in the mornings during the days of each analysis (Oyi, 2010).

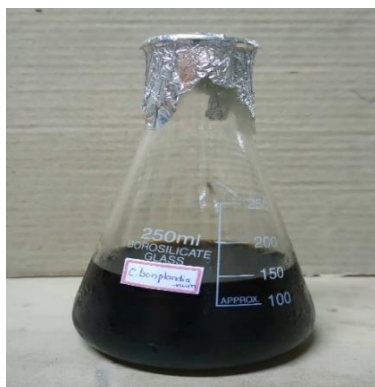


**Figure.2. Leaf Extract *Croton bonplandianum L***

**Synthesis of Ag-Ni bimetallic nanoparticles:**  $\text{AgNO}_3$  solution was prepared by dissolving 1.6987 g (10mM) of  $\text{AgNO}_3$  and 100 ml of distilled water in a 500 mL beaker. And  $\text{Ni}(\text{NO}_3)_2 \cdot 6\text{H}_2\text{O}$  aqueous solution was prepared separately by dissolving 2.9079 g (10mM) of  $\text{Ni}(\text{NO}_3)_2 \cdot 6\text{H}_2\text{O}$  in 100 mL distilled water. To the 80 mL of above prepared and filtered green aqueous leaf extract of *C. bonplandianum L* was added to the aqueous solution of silver nitrate. Then reaction mixture turned in to pale brown color. And to the separately prepared 100 mL of  $\text{Ni}(\text{NO}_3)_2$  solution were added drop wise in the simultaneous addition process. After this addition, the beaker was placed on a magnetic stirrer for continuous agitation and the mixture was stirred at  $80^\circ\text{C}$  for 90 minutes at pH 8. The pH of the

reaction medium could be adjusted by adding an adequate amount of 0.1 N HCl or 0.1 N NH<sub>4</sub>OH solutions. After 90 minutes the color of the reaction mixture is turned into dark brown color it conforms to the formation of the Ag-Ni bimetallic nanoparticles. These synthesized BMNPs were separated out by doing centrifugation at 5000 rpm for 50 minutes. The obtained BMNPs were washed with deionized water three times to remove unwanted constituents and dried in an oven at 70°C for three hours. The resultant Ag-Ni BMNMs particles were collected (Figure. 3) and used to further characterization.



**Figure.3. Preparation of Ag-Ni BMNPs from precursor solutions**

**Evaluation of antibacterial activity:** The antibacterial properties of produced Ag-Ni BMNPs were investigated using the agar -well diffusion method. The bacterial inoculation was made by growing one colony of *Escherichia coli* and *Staphylococcus aureus* in nutrient broth right away. On Mueller–Hinton agar (MHA) plates, 100µL of bacterial evaluation pathogens were spread, and various concentrations of Ag–Ni BMNPs (100, 200, 400 and 600 µg/mL) were inserted in colonies of a 5 mm dimension, then the plates were incubated for 24 hours at 37°C. An antibiotic zone scale was used to determine the inhibition zones. Ag–Ni BMNPs showed substantial antibacterial activity against both bacterial strains in a dose-dependent manner (100, 200, 400 and 800 µg/ml) in the comparison.

**Evaluation of Antifungal activity:** The agar well diffusion method was used to test the antifungal activity of green produced Ag-Ni bimetallic nanoparticles. The antifungal activity of Ag-Ni BMNPs was determined by inoculating the fungus in broth media and culturing them at 27°C for 72 hours. Plates of potato dextrose agar were made. Each Petri plate was injected with 10<sup>3</sup> spores per millilitre (0.1 ml) of solid media and dispersed evenly. Wells with a diameter of 6mm were drilled using a sterilized cork borer and then filled with 100mg/ml test samples. For positive and negative controls, an antifungal fluconazole disc (25mg drug concentration) and DMSO were used, respectively. And various concentrations of Ag–Ni BMNPs (20, 40, 60 and 80 µg/mL) were inserted in colonies of a 5 mm dimension, then the plates were incubated for an incubation chamber for 5-7 days at 27°C and then the diameter of the zone of inhibition was calculated (Balakumar, 2011).

**Anti-TB activity using Alamar Blue Dye:** Growth on Lowenstein Jensen (LJ) medium was suspended in sterile Middlebrook 7H9 broth supplemented with 0.2% glycerol and 10% OADC (oleate-albumin dextrose- catalase) enrichment and a 1:20 dilution used as the inoculum for MABA. All processing was conducted with suitable safety hoods. 200 µl of sterile deionized water was added to sterile 96 well plate outer perimeter wells to minimize medium evaporation during incubation in the test wells. The 96 well plate supplied 100 µl of the Middlebrook 7H9 broth, and compound serial dilution was made directly on the plate. The final drug concentrations tested were 25, 12.5, 6.25, 3.125, 1.56 and 0.78, 0.39, 0.19, 0.095, 0.047 µg/ml. Plates were covered and sealed with parafilm and incubated at 37 °C for five days. After this time, 25 µl of freshly prepared 1:1 mixture of Alamar Blue reagent and 10% tween 80 was added to the plate and incubated for 24 hrs. A blue color in the well was interpreted as no bacterial growth, and pink colour was scored as growth. The MIC was defined as the lowest drug concentration which prevented the colour change from blue to pink.

**Characterization:** Formation of Ag-Ni BMNPs was confirmed by UV-Visible absorption spectra using UV-2450 SHIMADZU double beam spectrophotometer, FTIR using Bruker, SEM, EDX studies are done by using Hitachi S-3700N machine and the morphology of BMNPs was elucidated by HRTEM analysis with FEI Technai machine.

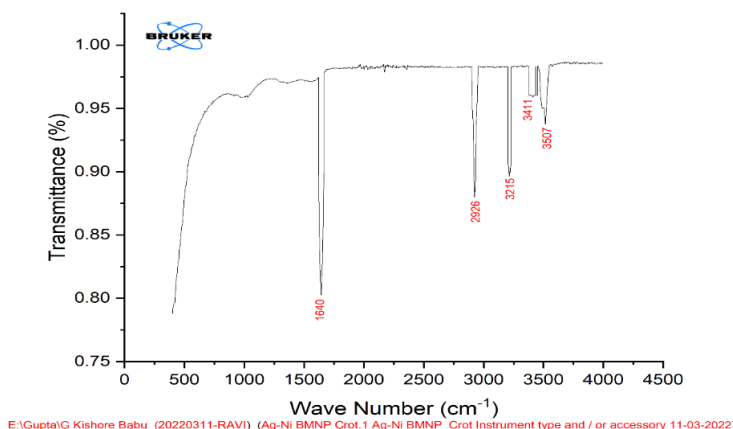
### 3. RESULTS AND DISCUSSION

**UV-Visible spectral analysis:** Visible absorption spectrum of Ag-Ni BMNPs is presented in Figure 4. The characteristic surface plasmon resonance (SPR) band at around 438 nm is observed in Ag-Ni BMNPs which confirms the nano size of the synthesized BMNPs (Zheng and Lombardi, 2008).



**Figure.4. UV-Visible absorption spectrum of Ag-Ni BMNPs**

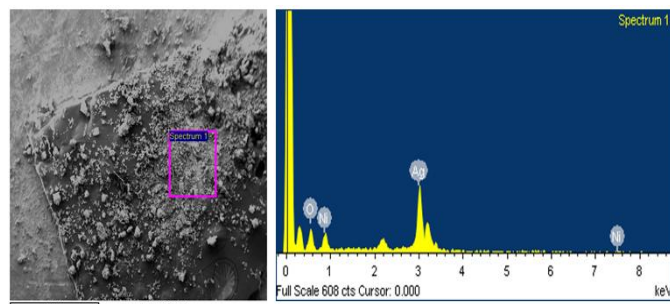
**FTIR spectroscopic analysis:** FTIR spectral data is used to reveal different functional groups present in biomolecules of *C. bonplandianum L* leaf extract. These biomolecules act as capping agents and these groups are responsible for the bioreduction of  $\text{Ag}^+$ ,  $\text{Ni}^{+2}$  precursors to  $\text{Ag}^{(0)}$ ,  $\text{Ni}^{(0)}$  and also for capping and stabilization of Ag-Ni BMNPs. The intense peaks were observed and compared with standard values to analyze the functional groups in *C. bonplandianum L* leaf extract and green synthesized Ag-Ni BMNPs. FTIR spectrum of synthesized Ag-Ni BMNPs by using *C. bonplandianum L* leaf extract was given in Figure 5. The comparison of the FTIR spectra of both Ag-Ni BMNPs and leaf extract of *C. bonplandianum L* clearly indicates the existence of the plant extract phyto molecules such as terpenes, flavonoids, polyphenols, glycosides, carbohydrates, tannins, amides, amines, sterols on the surface of the Ag-Ni BMNPs.



**Figure.5. FTIR spectrum of Ag-Ni BMNPs**

The N-H stretching vibrations of amines and O-H stretching vibrations of hydroxyl groups of alcohols and phenols are shown by prominent peak locations at  $3215\text{ cm}^{-1}$ ,  $3507\text{ cm}^{-1}$ , and  $3411\text{ cm}^{-1}$  in the FTIR spectrum of Ag-Ni BMNPs. The C=O stretching of the amide group results in a strong peak at  $1640\text{ cm}^{-1}$ . C-H stretching in the alkyl group is seen by the sharp peak at  $2926\text{ cm}^{-1}$ . Because the phyto molecules in the leaf extract act as bio reducing agents, capping and stabilizing agents for the produced nanoparticles, FTIR analysis clearly confirms that all of the previously mentioned absorption peaks of the leaf extract are barely shifted in the FTIR spectrum of Ag-Ni BMNPs. Biodegradable, well-distributed, biosoluble, biocompatible, and non-toxic capping agents are ideal. Capping agents improve the biological characteristics of nanoparticles. The presence of these IR peaks in Ag-Ni BMNPs demonstrated that plant secondary metabolites such as carbohydrates, glycosides, Saponin, phytosterols, phenols, tannins, flavonoids, proteins, amino acids, terpenoids, carboxylic acids, amides, carbonyl compounds, and alkyl were present on the nanoparticles' surface (Nimisha and Rani, 2019).

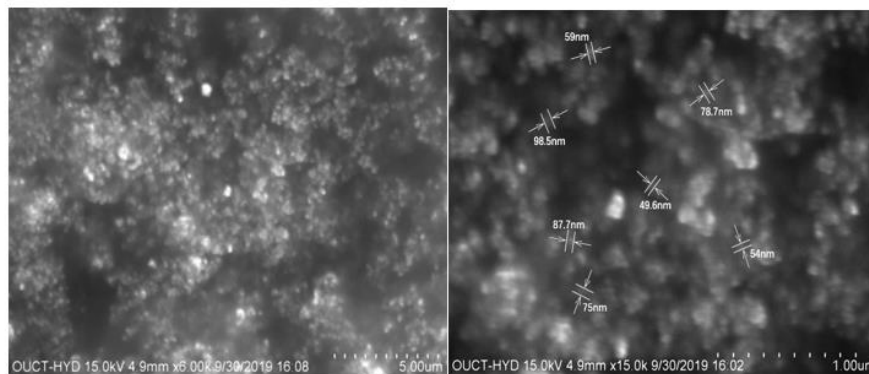
**Field Emission Scanning Electron Micrographs (FESEM) and EDX analysis:** We can examine all the components included in the BMNMs generated by *C. bonplandianum L* leaf extract using energy dispersive X-ray analysis. Figure 6 and Table 1 shows EDX spectrum and elemental composition respectively. This indicates the presence of the elements of Ag and Ni which confirms the formation of Ag-Ni bimetallic nanomaterials. This is also supported by the EDX is a study that provides quantitative data of silver and nickel compositions in BMNPs. From the EDX study, some parts of the Ag-Ni BMNPs appeared to be in the form of Ag-Ni Oxide caused by the presence of an excess of oxygen. This could be due to the open reaction system of the synthesis process in the present study. Figure 6 shows FESEM images of silver-Nickel BMNPs at different magnification. The synthesized Ag-Ni bimetallic nanoparticles are obviously in the size range from 50 to 100 nm size, as can be seen from this. The reduced nanoparticles with lower size show the potential reducing property of the *C. bonplandianum L* leaf extract for the synthesis of bimetallic nanoparticles. Table 1 and Figure 6 shows the elemental composition of the synthesized nanoparticles.



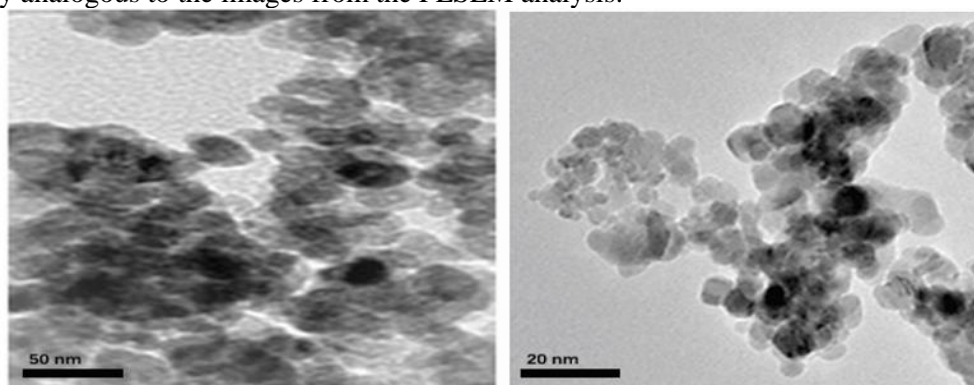
**Figure.6. EDX analysis of Ag-Ni BMNPs**

**Table.1. Quantitative results of Ag-Ni BMNPs**

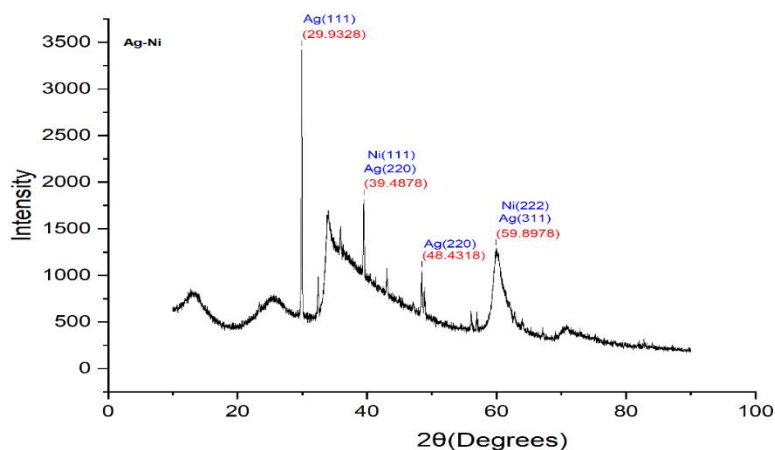
Element	Weight %	Atomic %
Ni	16.18	16.95
Ag	73.06	41.67
O	10.76	41.38
Totals	100.0	100.0

**Figure.7. FESEM images of Ag-Ni BMNPs**

**High-Resolution Transmission Electron microscopy analysis (HRTEM):** High-resolution transmission electron microscopy (HRTEM) pictures of produced Ag-Ni bimetallic nanoparticles from *C. bonplandianum L* (CB) leaf extract is shown in Figure 8. Ag-Ni BMNPs with spherical morphology and crystalline structure less than 100 nm in size were observed in these photos. Furthermore, the two metal nanoparticles seem to be in close proximity to one another. It's very analogous to the images from the FESEM analysis.

**Figure.8. HRTEM images of Ag-Ni BMNPs**

**Powder XRD analysis:** Figure 9, shows the XRD spectrum of green produced Ag-Ni BMNPs from CB leaf extract. The peaks at  $2\theta$  values of  $29.930^\circ$ ,  $39.480^\circ$ ,  $48.430^\circ$ , and  $59.890^\circ$  correspond to Bragg's reflections of Ag (111), Ag (220), Ni (111), Ag (220), Ni (222), and Ag (311) planes of face-centered cubic crystal structure (Sridharan, 2013).

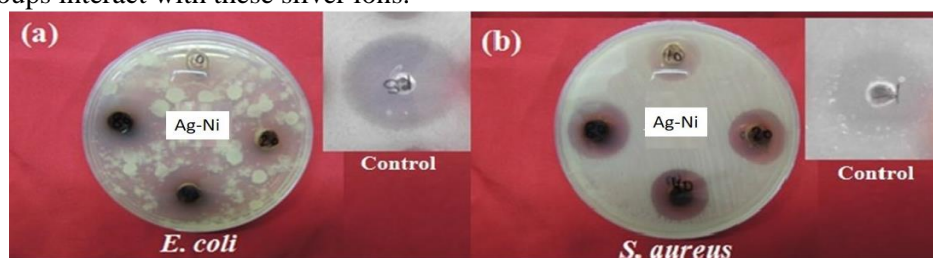
**Figure.9. XRD spectrum of Ag-Ni BMNPs**

**Table.2. Crystalline sizes of Ag-Ni BMNPs**

S.No.	2 $\theta$ (degrees)	$\theta$ (radians)	Cos $\theta$	B (radians)	D (nm)
1	29.93 <sup>0</sup>	0.5223	0.8667	0.00714	22.40673
2	39.48 <sup>0</sup>	0.6891	0.7719	0.00664	27.0551
3	48.43 <sup>0</sup>	0.8453	0.6653	0.00686	30.46231
4	59.89 <sup>0</sup>	1.0452	0.5018	0.00673	41.06277

The values of crystalline sizes for different 2 $\theta$  values were calculated as per the Debye-Scherrer equation and given in Table 2. The average particle size of the produced Ag-Ni BMNPs is 30.24672 nm, according to the numerically computed value.

**Evaluation of antibacterial activity:** Ag-Ni BMNPs had a considerable inhibitory impact and produced clearing zones of 20 and 21 mm against *S. aureus* and *E. coli* at a higher concentration of 600  $\mu\text{g/ml}$ . The inhibitory activity can be compared to that of traditional antibiotics, such as the clearance zones of 28 and 24 mm achieved in the presence of streptomycin. More specifically, the Ag-Ni BMNPs displayed a 10 and 6 mm zone of inhibition against *S. aureus* and *E. coli*, respectively, at a lower 100  $\mu\text{g/ml}$  concentration (Table 3). According to Feng (2008), and Matsumura (2003), reactive oxygen species (ROS) promote cell self-destruction. Because silver nanoparticles disintegrate into silver ions, ROS are produced as a result of the inactivation of respiratory enzyme chains. Several enzymes thiol groups interact with these silver ions.

**Figure.10. Representative results of anti-bacterial activity of Ag-Ni BMNPs****Table.3. Zone of inhibitions of Ag-Ni BMNPs and Streptomycin (controller) against *S.aureus* and *E.coli***

Bacterial strain	Concentrations( $\mu\text{g/mL}$ ) of Ag-Ni BMNPs				Streptomycin
	100 ( $\mu\text{g/mL}$ )	200 ( $\mu\text{g/mL}$ )	400 ( $\mu\text{g/mL}$ )	600 ( $\mu\text{g/mL}$ )	
<i>S.aureus</i> (Gram +ve)	10	17	18	20	28
<i>E. coli</i> (Gram -ve)	6	16	16	21	24

**Evaluation of Antifungal activity:** Ag-Ni BMNPs had a considerable inhibitory impact and produced clearing zones of 15.00 $\pm$ 0.5mm and 17.00 $\pm$ 0.5mm against *Aspergillus flavus* and *Candida albicans* at a higher concentration of 800  $\mu\text{g/ml}$ . More specifically, the Ag-Ni BMNPs displayed a 6.00 $\pm$ 0.5mm and 9.00 $\pm$ 0.5 mm zone of inhibition against *A.flavus* and *C.albicans*, respectively, at a lower 10  $\mu\text{g/ml}$  concentration. The antifungal drug Fluconazole is used as a standard and DMSO is negative control. Even at a lower 200  $\mu\text{g/ml}$  concentration Ag-Ni BMNPs displayed a 9.00 $\pm$ 0.5mm and 6.10 $\pm$ 0.5mm zone of inhibition against *A.flavus* and *C.albicans*, respectively.

**Table.4. Zone of inhibitions of Ag-Ni BMNPs and Streptomycin (controller) against *A.flavus* and *C.albicans***

Fungal strain	Concentrations ( $\mu\text{g/mL}$ ) of Ag-Ni BMNPs				Fluconazole disc	DMSO
	200 ( $\mu\text{g/mL}$ )	400 ( $\mu\text{g/mL}$ )	600 ( $\mu\text{g/mL}$ )	800 ( $\mu\text{g/mL}$ )		
<i>A. flavus</i>	9.00 $\pm$ 0.5mm	9.00 $\pm$ 0.5mm	12.00 $\pm$ 0.5mm	15.00 $\pm$ 0.5mm	16.78 $\pm$ 0.8mm	-
<i>C.albicans</i>	6.10 $\pm$ 0.5mm	9.00 $\pm$ 0.5mm	15.10 $\pm$ 0.5mm	17.00 $\pm$ 0.5mm	20.0 $\pm$ 0.8mm	-

**Figure.11. Representative results of anti-fungal activity of Ag-Ni BMNPs**

25 12.5 6.25 3.12 1.5 0.8 0.4 0.2 0.1 0.05



Figure.12. Inhibition activity of synthesized nanoparticles

Table.5. Inhibition activity of synthesized nanoparticles

SAMPLE	25	12.5	6.25	3.12	1.56	0.78	0.39	0.19	0.095	0.047
RC 1	S	S	R	R	R	R	R	R	R	R

The above analysis indicates the inhibition of bacterial growth by the tested sample RC1 is Ag-Ni, synthesized bimetallic nanoparticles. Even a very small dose of RC1 tested sample showed high inhibition of the bacterial growth at a low concentration of (12.5 µg/ml).

#### 4. CONCLUSION

An ecologically safe method is projected in this report to synthesize Ag-Ni bimetallic nanoparticles from *Croton blanfordinum* L leaf extract. From UV-VIS spectral analysis it is confirmed that the particles are in nano scale as per the positions of the Surface Plasmon Resonance (SPR) bands. FTIR data confirms the presence of secondary metabolites of phyto molecules that act as the bio reducing and capping agents of the formed nanoparticles. Results of XRD, SEM and TEM analyses proved that Ag-Ni BMNPs are in spherical morphology and cubic crystalline structure with size between 20-100 nm. Ag-Ni BMNPs had a considerable inhibitory impact and produced clearing zones of 20 and 21 mm against *S. aureus* and *E. coli* at a higher concentration of 600 µg/ml. and displayed a 10 and 6 mm zone of inhibition against *S. aureus* and *E. coli*, respectively, at a lower 100 µg/ml concentration. Even at a lower 200 µg/ml concentration Ag-Ni BMNPs displayed a 9.00±0.5mm and 6.10±0.5mm zone of inhibition against *A. flavus* and *C. albicans*, respectively. Green synthesized Ag-Ni BMNPs also showed inhibition of the *Mycobacterium tuberculosis* by using Alamar blue dye in the lowest concentration range of >12.5 µg/ml.

**Conflicts of interest:** We declare that we have no conflicts of interest.

#### 5. ACKNOWLEDGEMENT

Authors profusely UGC-RGNF (F1-17.1/2016-17/RGNF-2015-17-SC-AND-9605/(SA-III)), for supporting financially throughout the work. Instrumentation help was provided by IPE, Visakhapatnam, Pharmaceutical Sciences, Andhra University, Visakhapatnam.

B. Kishore babu and K. Mohana Rao acknowledges grants from the Ref No: 42-354/2013 UGC (INDIA), New Delhi. We are grateful for the technical assistance provided by the Department of Engineering Chemistry at the Andhra University, Visakhapatnam (India) and the University of Hyderabad for providing the spectral data.

#### REFERENCES

- Balakumar S, Rajan S, Thirunalasundari T, Jeeva S, Antifungal activity of *Ocimum sanctum* Linn. (Lamiaceae) on clinically isolated dermatophytic fungi, *Asian Pac J Trop Med.*, 4 (8), 2011, 654-657.
- Chandel Anuj K, Silva Silvio S, Singh Om, Detoxification of Lignocellulosic Hydrolysates for Improved Bioethanol Production, *Biofuel Production*, 2011.
- Daniel MC, Astruc D, Gold nanoparticles: assembly, supramolecular chemistry, quantum size-related properties, and applications toward biology, catalysis, and nanotechnology, *Chemical Reviews*, 104 (1), 2004, 293-346.
- Divya B, Kenganora Mruthunjaya and Manjula S.N, *Parkinsonia aculeata*: A Phytopharmacological Review, *Asian Journal of Plant Sciences*, 10 (3), 2011, 175-181.
- Feng Q.L, Wu J, Chen G.Q, Cui F.Z, Kim T.N, Kim J.O, A mechanistic study of the antibacterial effect of silver ions on *Escherichia coli* and *Staphylococcus aureus*, *J. Biomed. Mater. Res.*, 52 (4), 2000, 662-668.
- Greer JR, and Nix WD, Nanoscale gold pillars strengthened through dislocation starvation, *Phys. Rev B*, 73 (24), 2006.

Jeeshna M.V, Paulsamy S, and Mallikadevi T, Phytochemical Constituents and Antimicrobial Studies of the Exotic Plant Species, *Croton bonplandianum* Baill, Journal of Life Sciences, 3 (1), 2011, 23-27.

Kaehler T, Nanotechnology: basic concepts and definitions, Clin. Chem., 40 (9), 1994, 1797–1799.

Koduru J.R, Kailasa S.K, Bhamore J.R, Kim K.H, Dutta T, and Vellingiri K, Phytochemical-assisted synthetic approaches for silver nanoparticles antimicrobial applications: A review, Advances in Colloid and Interface Science, 256, 2018, 326–339.

Lee J, Park E.Y, and Lee J, Non-toxic nanoparticles from phytochemicals: preparation and biomedical application, Bioprocess and biosystems engineering, 37 (6), 2014, 983-989.

Maksakova O.V, Webster R.F, Tilley R.D, Ivashchenko V.I, Postolnyi B.O, Bondar O.V, and Pogrebnjak A.D, Nanoscale architecture of (CrN/ZrN)/(Cr/Zr) nanocomposite coatings: Microstructure, composition, mechanical properties and first-principles calculations, Journal of Alloys and Compounds, 2020, 154808.

Mansoori GA, Soelaiman TAF, Nanotechnology- an introduction for the standards community, Journal of ASTM International, 2 (6), 2005, 1-21.

Matsumura Y, Yoshikata K, Kunisaki S, Tsuchido T, Mode of bactericidal action of silver zeolite and its comparison with that of silver nitrate, Appl. Environ. Microbiol. 69 (7), 2003, 4278–4281.

Nimisha S, and Rani K.B, Antibacterial activity and phytochemical screening of ethanolic leaf, stem and flower extract of *Aerva lanata*. Journal of Applied and Natural Science, 11 (2), 2019, 455-461.

Oyi A.R, Onaolapo J.A, and Obi R.C, Formulation and Antimicrobial Studies of Coconut (*Cocos nucifera* Linne) Oil, Research Journal of Applied Sciences, Engineering and Technology, 2 (2), 2010, 133-137.

Pantidos N, Biological Synthesis of Metallic Nanoparticles by Bacteria, Fungi and Plants, Journal of Nanomedicine & Nanotechnology, 5 (5), 2014.

Park Y, Hong Y.N, Weyers A, Kim Y.S, and Linhardt R.J, Polysaccharides and phytochemicals: a natural reservoir for the green synthesis of gold and silver nanoparticles, IET nano biotechnology, 5 (3), 2011, 69-78.

Parthiban A, Sivasankar R, Sachithanandam V, Ajmal Khan S, Jayshree A, Murugan K, Sridhar R, An integrative review on bioactive compounds from Indian mangroves for future drug discovery, South African Journal of Botany, 2021.

Sahoo A, Singh B, Bhat T.K, Effect of tannins on *in vitro* ruminal protein degradability of various tree forages, Livestock Research for Rural Development, 22 (7), 2010.

Selvamangai G and Bhaskar Anusha, GC–MS analysis of phytocomponents in the methanolic extract of *Eupatorium triplinerve*, Asian Pacific Journal of Tropical Biomedicine, 2 (3), 2012, S1329–S1332.

Shah M, Fawcett D, Sharma S, Tripathy S.K, and Poinern G.E.J, Green synthesis of metallic nanoparticles via biological entities, Materials, 8 (11), 2015, 7278-7308.

Sirdeshpande K.D, Sridhar A, Cholkar K.M, and Selvaraj R, Structural characterization of mesoporous magnetite nanoparticles synthesized using the leaf extract of *Calliandra haematocephala* and their photocatalytic degradation of malachite green dye, Applied Nanoscience, 8 (4), 2018, 675–683.

Sridharan K, Endo T, Cho S.G, Kim J, Park T.J, and Philip R, Single step synthesis and optical limiting properties of Ni–Ag and Fe–Ag bimetallic nanoparticles, Optical Materials, 35 (5), 2013, 860–867.

Srinoi P, Chen Y.T, Vittur V, Marquez M.D, and Lee T.R, Bimetallic Nanoparticles: Enhanced Magnetic and Optical Properties for Emerging Biological Applications, Applied Science, 8 (7), 2018, 1106.

Venkatesan P, and Santhanalakshmi J, Core-Shell Bimetallic Au-Pd Nanoparticles: Synthesis, Structure, Optical and Catalytic Properties, Nanoscience and Nanotechnology, 1 (2), 2011, 43–47.

Zheng X, and Lombardi J, Light-induced growth of monodisperse silver nanoparticles with tunable SPR properties and wavelength self-limiting effect, Plasmonics: Metallic Nanostructures and Their Optical Properties VI, 7032, 2008.